

Neural correlates of motor memory with multiple time scales in sensorimotor adaptation

Sung Shin Kim, Kenji Ogawa, Jinchi Lv, Nicolas Schweighofer, Hiroshi Imamizu

Recent behavioral studies with computational models have revealed motor memory with multiple time scales in sensorimotor adaptation [1]. However, little has been studied about underlying neural correlates of the motor memory. For this, we designed an even-related fMRI experiment where 21 subjects (15 males and 6 females) learned opposing visuomotor rotation (40° or -40°) tasks in alternating blocks by which we could prevent premature adaptation within few trials. Then, the traces of motor memory activation with 30 different time scales, logarithmically scaled from 2 s to 92.6 h, were estimated using a computational model as described below [1]. To account for dual adaptation, we defined the state of motor memory with a time constant, τ_k as a vector with two internal states. $\mathbf{x}_k = [x_{k,1} \ x_{k,2}]^T$. The motor adaptation at each trial, n is given by the sum of the 30 states of memory. The update equation of the memory state with a time constant, τ_k is given as

$$\mathbf{x}_k(n+1) = \mathbf{x}_k(n)e^{-T(n)/\tau_k} + \beta_k \cdot e(n) \cdot \mathbf{c}(n), \quad \beta_k = \frac{c}{\tau_k^p} (k = 1, 2, \dots, 30)$$

where \mathbf{c} is the contextual cue addressing the two internal states such that $\mathbf{c} = (1 \ 0)^T$ for Task 1 (40°) and $\mathbf{c} = (0 \ 1)^T$ for Task 2 (-40°). The states of motor memory decays exponentially as time and are updated for each trial at the moment of receiving error feedbacks, $e = f - y$ where y is a motor output and f is an external perturbation, i.e., visuomotor rotations. The fitted parameters of the proposed model were : $c = 0.0487$ and $p = 0.263$ with an overall fitting performance as a mean absolute error, 3.06° . Each of the 30 estimated states shown in Fig. 1 was used as a regressor in the general linear model. Fig. 2 shows correlated brain regions with each of regressors with different time scales, using generous significance level ($p < 0.001$) for explorative purpose. Further multiple comparison and region of interest (ROI) analysis were performed and summarized in a separate table.

We additionally conducted a multi-voxel pattern analysis (MVPA) to test if the regional brain activity could be used to classify the two rotational types. The ROIs include the right parietal lobe and the cerebellum (Fig. 3a). Within the ROIs, we applied MVPA to BOLD signals of voxels that were significantly correlated with at least one of the intermediate components (τ_k , ranged from 2.1 to 87.9 minutes: $k = 11, \dots, 20$) in the model-based regression analysis. In the cerebellum, MVPA was applied to signals that were significantly correlated with at least one of the slow components (τ_k , ranged from 2.2 to 92.6 hours: $k = 21, \dots, 30$). The classification was performed with a linear support vector machine. The one-way analysis of variance with sessions as an intra-subject factor revealed significant increase of accuracy in the cerebellum ($p < 0.001$), but no significant difference in the right aIPPL ($p > 0.05$) (Fig. 3b). These results indicate that specificity of activity patterns to the task (40 or -40° rotations) increased with sessions in the cerebellum. We further confirmed that the increase in classification accuracy with session observed in the cerebellum is not due to behavioral confounds during adaptation (Fig. 3c).

In sum, we searched over neural correlates of motor memories with varying time scales during motor adaptation. The correlated brain regions shifted from the fronto-parietal area down to the cerebellar area, correspondingly from the fastest to the slowest time constants. The MVPA result provides supplementary evidence that the cerebellum is a site for the multiple slow processes learning separate representation of dual adaptation and this is consistent with the results of a previous study [2].

[1] Kording, K.P. et al., *Nat Neurosci*, 10, 779-786, 2007.

[2] Imamizu, H. et al., *Proc Natl Acad Sci U S A*, 100, 5461-5466, 2003.

Acknowledgements: The modeling work of this study was supported by NSF BCS 1031899 to NS

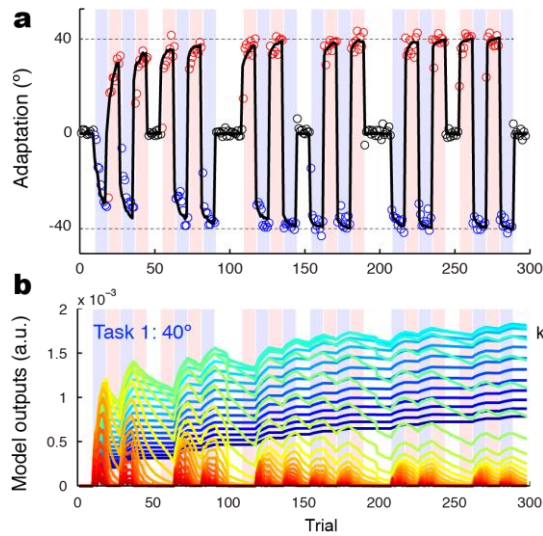


Figure 1. Adaptation process in behavioral data and result of model fitting. (a) Blue, red, and black circles indicate direction of joystick movements in Task 1 (40° visuomotor rotation), Task 2 (-40°), and Control (0°), respectively, averaged across subjects (N = 21). Blue or red shaded regions indicate trials in Task 1 or 2, respectively. A thick black line indicates total output of multi-state model. (b) Profiles of individual states of motor memory for Task 1 of the fitted model. Colors indicate component numbers (k) and corresponding time constants (τ_k) as indicated by the color bar.

Figure 2. Correlated regions for individual states of motor memory with 30 different time constants. (a) Red-yellow regions indicate those where BOLD signal time courses were significantly correlated with those of individual states of motor memory (see Fig. 1b) ($p < 0.001$ uncorrected for multiple correction). Color-coded T -values of regression coefficients are rendered on right posterior view of the brain surfaces. Blue circles indicated the anterior regions of inferior parietal lobe and the cerebellum, which are consistently responsible for intermediate ($k = 11, \dots, 20$) and slow components ($k = 21, \dots, 30$). (b) Regional difference in the cerebellum between the fastest ($k = 1$) and slowest ($k = 30$) components. ReSgions related to each component are indicated in the transverse sections the superior (the left panel) to the inferior (the right panel) sections.

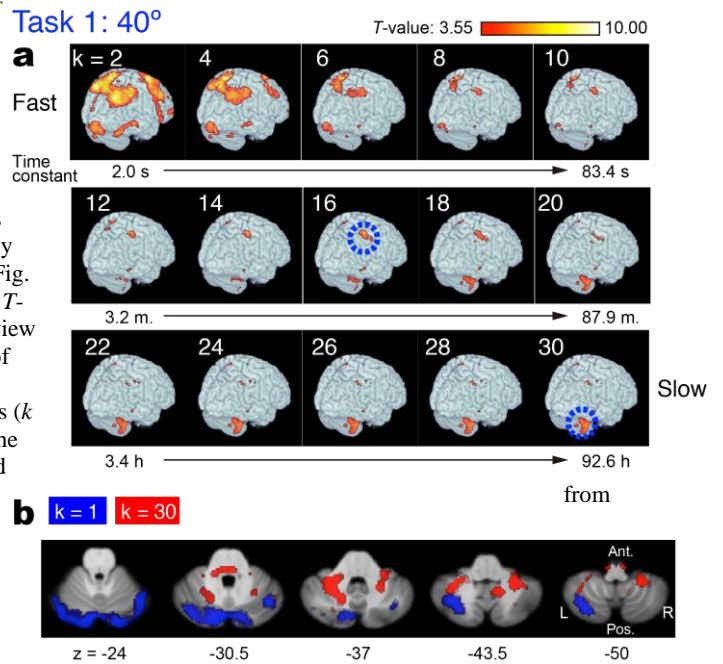


Figure 3. Regions of interest (ROIs) and classification accuracy of multi-voxel pattern analysis. (a) Functional ROIs to which multi-voxel pattern analysis was applied (gray-black regions). Broken lines indicate anatomical ROIs (red: the superior and the inferior parietal lobes, and cyan: the cerebellum). Right and the left panels indicate the parietal and cerebellar ROIs, respectively. Top and bottom panels shows the regions projected to the sagittal and the transverse planes, respectively. (b) Classification accuracy of Task 1 and 2 as a function of sessions using activity patterns in the above functional ROIs. A plus (+) marker indicates accuracy averaged within each subject according to cross-validation tests. Thick lines indicate accuracy averaged across subjects. The one-way analysis of variance with sessions as a intra-subject factor revealed significant increase of accuracy in the cerebellar ROI ($p < 0.001$), but no significant difference in the parietal ROI ($p > 0.05$). (c) Variance (standard deviation: SD) of directional error among trials in a session for individual subjects (gray circles). Red lines and boxes indicate mean and SD of the SDs in each session. Significant difference of SD in errors was found between the 1st and 2nd sessions ($p < 0.01$ [*: $p < 0.02$ corrected for two comparisons with Bonferroni method]), but no significant difference between the 2nd and 3rd sessions ($p = 0.82$, ns: not significant)

